

Lateral Diffusion Length Changes in HgCdTe Detectors in a Proton Environment

John E. Hubbs, *Member, IEEE*, Paul W. Marshall, *Member, IEEE*, Cheryl J. Marshall, Mark E. Gramer, Diana Maestas, John P. Garcia, Gary A. Dole, and Amber A. Anderson

Abstract—This paper presents a study of the performance degradation in a proton environment of long wavelength infrared (LWIR) HgCdTe detectors. The energy dependence of the Non-Ionizing Energy Loss (NIEL) in HgCdTe provides a framework for estimating the responsivity degradation in LWIR HgCdTe detectors due to on-orbit exposure from protons. Banded detector arrays of different detector designs were irradiated at proton energies of 7, 12, and 63 MeV. These banded detector arrays allowed insight into how the fundamental detector parameters degraded in a proton environment at the three different proton energies. Measured data demonstrated that the detector responsivity degradation at 7 MeV is 5 times larger than the degradation at 63 MeV. Comparison of the responsivity degradation at the different proton energies suggests that the atomic Coulombic interaction of the protons with the HgCdTe detector is likely the primary mechanism responsible for the degradation in responsivity at proton energies below 30 MeV.

Index Terms—HgCdTe detectors, Non-Ionizing Energy Loss (NIEL), proton radiation effects.

I. INTRODUCTION

SPACE-BASED infrared imaging systems place stringent performance requirements on long wavelength infrared (LWIR) detectors in terms of sensitivity, uniformity, operability, and radiation hardness. The radiation hardness goals for these systems are typically dominated by proton interactions with the hybrid detector array. The three sources of protons impacting space-based detector arrays are: 1) protons in the inner Van Allen radiation belt; 2) the proton component of solar particle events; and 3) hydrogen nuclei from intergalactic cosmic rays. Transient signatures of proton ionization in LWIR HgCdTe hybrid detectors have been investigated and reported in [1]. Proton interaction with the HgCdTe-based hybrid detectors also

results in permanent performance degradation, primarily due to total ionizing dose (TID) effects and displacement damage effects. TID effects are generated by the loss of the kinetic energy from an incident proton to ionization, and primarily degrade the operation of Si readout integrated circuits (ROIC) through flat-band voltage shifts and increased leakage currents. Displacement damage effects result when proton energy is lost to non-ionizing processes, causing atoms to be removed from their lattice sites and form permanent electrically active defects. These displacement damage effects primarily degrade the performance of the HgCdTe detector array through increased dark current, reduction in responsivity, and degraded uniformity.

Recent measured results from exposing LWIR HgCdTe detector arrays [2] to proton radiation have shown a decrease in responsivity with increasing proton fluence. The loss in responsivity has been isolated to the detector, and its root cause is related to the detector design. The detector design relies on lateral collection of charge to achieve high performance in quantum efficiency; this reliance on lateral collection causes the loss of responsivity in a proton environment. A major consideration in LWIR HgCdTe detector design is the diameter of the lateral collection diode implant, which directly affects the noise, responsivity, sensitivity, operability, and tolerance to proton fluence. If the diode diameter is large, the responsivity (detector quantum efficiency) will be maximized, but at the expense of degraded operability due to the increased probability of intersecting a defect. In addition, a detector with a large diode diameter relies less on lateral collection of charge and is thus more tolerant to interactions with protons. At the other extreme, a small lateral collection diode optimizes detector array operability, but the responsivity, and consequently the sensitivity, is degraded. A detector with a small implant diameter requires a long lateral collection length to achieve reasonable responsivity (quantum efficiency); therefore, its performance will degrade if the lateral collection length is compromised in a proton environment. Thus, for this type of detector design, a trade space exists that balances the responsivity and sensitivity performance against operability and proton fluence performance.

This study investigates the change in LWIR HgCdTe detector responsivity and lateral collection length in a proton environment, with the goal of obtaining data to support the development of an on-orbit performance estimation tool for these detector arrays. This analysis assumes that the dominant cause of detector performance change is displacement damage resulting from protons interacting with the HgCdTe detectors. The estimation tool will utilize the concept of non-ionizing energy loss rate (NIEL) in HgCdTe, which is due to Coulombic, nuclear elastic, and nuclear inelastic interactions between the protons

Manuscript received July 20, 2007; revised September 4, 2007. This work was supported in part by the Space Vehicles Directorate of the United States Air Force Research Laboratory and the NASA Electronic Parts and Packaging Program (NEPP).

J. E. Hubbs, M. E. Gramer, D. Maestas, J. P. Garcia, and G. A. Dole are with the Ball Aerospace & Technologies Corp., Albuquerque, NM 87185 USA (e-mail: jhubbs@ieee.org).

P. W. Marshall is a Consultant, Brookneal, VA 24528 USA (e-mail: pwmarshall@aol.com).

C. J. Marshall is with the NASA Goddard Space Flight Center, Greenbelt, MD 20771 USA (e-mail: cmarshall2@aol.com).

A. A. Anderson is with the Space Vehicles Directorate of the Air Force Research Laboratory (AFRL/VSSS) Kirtland AFB, NM 87117 USA (e-mail: amber.anderson@kirtland.af.mil).

Color versions of one or more of the figures in this paper are available online at <http://ieeexplore.ieee.org>.

Digital Object Identifier 10.1109/TNS.2007.910329

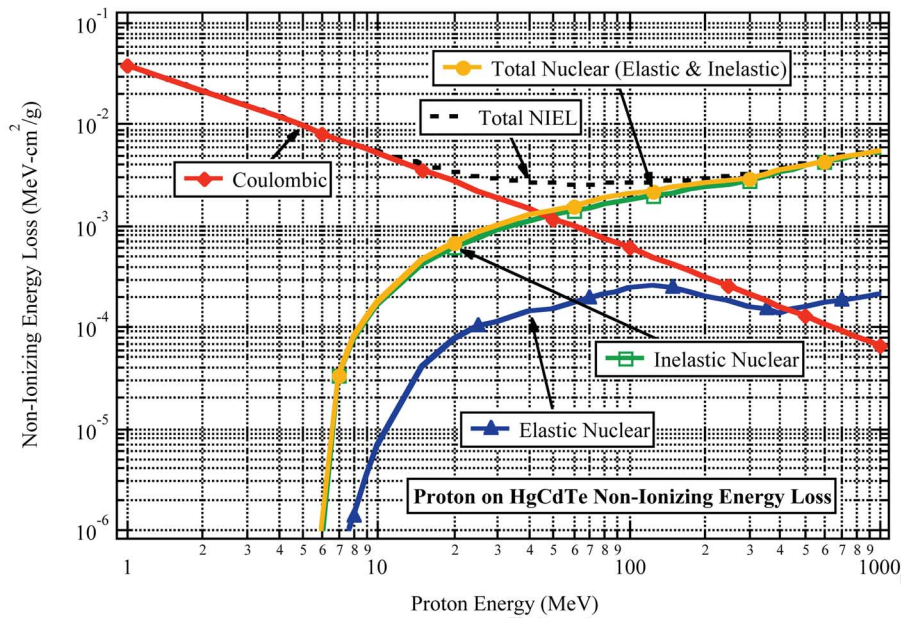


Fig. 1. Non-ionizing energy loss for protons on HgCdTe.

and the HgCdTe detector material. The energy dependence of the NIEL in HgCdTe provides a framework for estimating the on-orbit change in detector responsivity. This model development assumes that displacement damage is linear with proton fluence, and that damage in the detectors has the same energy dependence as NIEL—assumptions that will be evaluated by measurements in this study.

The detectors utilized in this study are banded LWIR HgCdTe detector arrays with varying diameters of single implant lateral collection diode designs. These banded detector arrays allow insight into how the fundamental detector parameters degrade in a proton environment. For these experiments, the proton response of the banded detector arrays was measured at proton energies of 7, 12, and 63 MeV.

II. NON-IONIZING ENERGY LOSS (NIEL) CONCEPT

This section briefly describes the methods used to compute the proton NIEL in HgCdTe. This computation methodology follows the treatment initially presented for calculating the NIEL for short-wave and midwave detectors [3]. NIEL has two components: 1) atomic Coulombic interactions and 2) nuclear interactions. Details on the methodology to compute the Coulomb contribution to proton NIEL can be found in [4]–[6]. The details of the calculation of the nuclear contributions to the proton NIEL using the Monte Carlo N-Particle eXtended (MCNPX) charged particle transport code can be found in [7], [8].

The proton NIEL was calculated for Hg, Cd, and Te, and the results were used to obtain the NIEL for the compound material by adding the results for the individual elements weighted by their stoichiometric ratios. Fig. 1 provides the results of these calculations and shows the separate contributions from nuclear elastic and inelastic interactions, as well as the atomic Coulombic interactions. Below 10 MeV, Coulombic interactions dominate the production of displaced atoms, while the

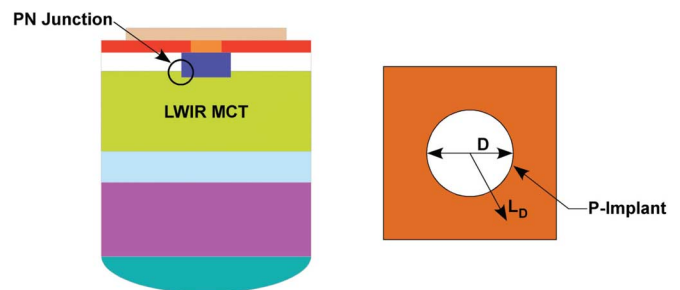


Fig. 2. LWIR HgCdTe detector structure.

nuclear collisions (particularly the nuclear inelastic) take over at energies above 30 to 50 MeV.

There are two primary aspects of the damage that may be expected to correlate with the calculated proton-induced NIEL. The first is damage-induced detector performance change as a function of proton energy, which results in a reduction in the lateral collection length leading to a change in detector responsivity. Numerous studies have shown the importance of understanding the energy dependence of damage as a key to relating the measured damage factors in the laboratory at a few discrete energies to the expected detector response to an orbital spectrum of proton energies [9]. The second aspect is the detector-to-detector variation in dark current. NIEL calculations can be extended to look at the second moment of non-ionizing energy deposition, and examined to describe this problem in terms of variations in the deposited damage energy [10].

III. EXPERIMENT

A. Description of LWIR HgCdTe Detector

The LWIR HgCdTe detectors were grown by molecular-beam epitaxy (MBE) on CdZnTe substrates using a p-on-n design. The detectors are single-implant lateral collection diode designs, with the implant centered in the pixel, coupled with a micro-lens structure, as shown in Fig. 2.

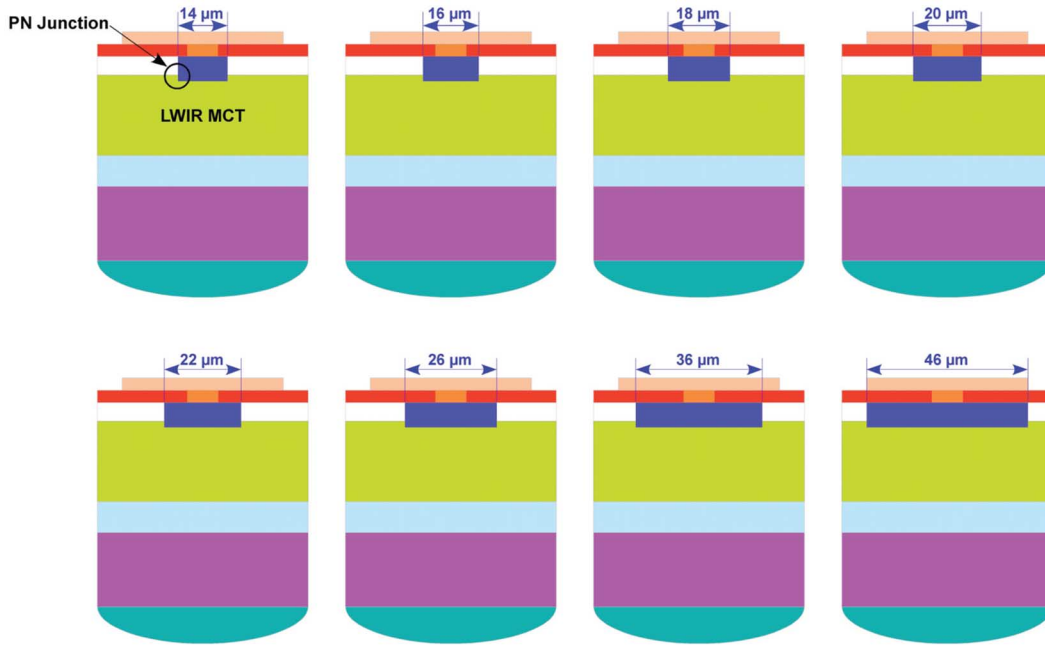


Fig. 3. LWIR HgCdTe banded array detector description showing implant size variation.

This detector design approach is used to improve the R_0A , which is the dynamic resistance of the detector at zero bias and is a measure of the detector dark current, and operability of the detector array. The detector arrays are anti-reflection (AR) coated to improve quantum efficiency at long wavelengths. The LWIR HgCdTe detector array has a cut-off wavelength greater than $11.0 \mu\text{m}$. Details of the detector design, the application of lateral collection concepts, and the application of microlens technology to LWIR HgCdTe detectors have been previously described [11]–[14].

This detector array used in this study is made up of eight different detector designs, with each design having 2048 pixels in the array. The principal design variation for the detector diodes is the diameter of the single implant, which varied from 14 to $46 \mu\text{m}$, as shown in Fig. 3. The eight detector designs are banded to incorporate the different single implant lateral collection diode designs into a single detector array. Banded detector arrays are used to help select the optimal detector design for a given pixel size by evaluating the tradeoff between lateral collection diode implant diameter and operability. Recall that a large diode diameter maximizes detector responsivity (quantum efficiency) and responsivity uniformity at the expense of degraded operability, while a small lateral collection diode offers improved operability and high detector R_0A , but at the expense of lower responsivity, lower sensitivity, and degraded uniformity.

A finite element model of LWIR HgCdTe detectors has been developed [15] to predict detector responsivity as a function of the minority carrier lateral collection length. This model incorporates several of the design features of the lateral collection detectors including the micro-lens structure. This model also allows evaluation of the impact of changes in the minority carrier lateral collection length on the detector quantum efficiency, spectral response, and other performance parameters.

The model's output consists of detector responsivity (normalized to responsivity of the detector with the largest implant) as a function of implant diameter and permits evaluation of the performance impact resulting from changes in the implant diameter and lateral collection length (L_D). Modeling results indicate that as the implant diameter decreases, the detector responsivity decreases. This model, described in more detail later in this section, also demonstrates that the detector responsivity has an approximate quadratic dependence on the lateral collection length. These modeling results provide insight into the damage mechanism in a proton radiation environment.

B. Proton Irradiation

Proton fluence measurements were performed at the University of California, Davis (UC Davis) Crocker Nuclear Laboratory (CNL). This proton beam facility is based on a $76''$ Isochronous Cyclotron that can provide protons with energies up to 68 MeV [16]. For these experiments, the cyclotron was configured to irradiate the LWIR HgCdTe detector array at proton energies of 63, 12, and 7 MeV.

The detector array was fully biased and operational at the nominal operating temperature of 40 Kelvin during proton irradiation. The detector arrays were subjected to a series of six proton irradiations, at each proton energy, to achieve total ionizing dose levels of 10, 20, 50, 100, 200, and 300 krad(Si). After each proton irradiation, the detector array was radiometrically characterized to determine the responsivity of each detector design.

C. Experiment Design

LWIR HgCdTe detectors collect charge from both the implanted area of each detector and from a volume of material around the implant by means of lateral collection. The active

detector area is a combination of the implant diameter and the lateral collection length as given by

$$A_{\text{Det}} = \pi(r + L_D)^2 \quad (1)$$

where r is the radius of the circular implant and L_D is the lateral collection length. The detector signal current is then determined by

$$i = q\eta E_q A_{\text{Det}} = q\eta E_q \pi(r + L_D)^2 \quad (2)$$

where q is the electron charge (C), η is the detector quantum efficiency, E_q is the photon irradiance at the detector, and A_{Det} is the active detector area. For any lateral collection length, the percentage of charge collected in this manner will be larger for smaller implant diameters, making the responsivity from the smaller implants more sensitive to changes in the lateral collection length. In a proton environment, the lateral collection length will likely degrade due to a decrease in the minority carrier lifetime with increasing proton radiation fluence, causing a decrease in the volume of the detector material from which charge can be collected. The detector responsivity will degrade in a proton environment because both the effective area and pixel thickness are decreased.

The lateral collection length is typically determined by measuring the photo-generated signal from variable area detector as a function of detector area. The lateral collection length is then determined from these data by plotting the square root of the detector current (\sqrt{i}) as a function of the detector implant diameter (r), fitting a straight line to the measured data that extends to the abscissa. The lateral collection length is where the fitted line intersects the abscissa. This is a common technique used in evaluating material quality of infrared detectors; however, it does not strictly apply to these detectors.

This type of analysis is complicated for LWIR HgCdTe detectors because of the micro-lens incorporated into the detector structure. Flood illumination is assumed in the analysis; however, the micro-lens tends to focus the light onto the center of the detector structure with a spot size of approximately 25 to 40 μm . The exact value of the spot size is dependent on the wavelength of light and the F/# (F number) of the micro-lens. A further complication arises due to the limited extent of the pixels. If the sum of the lateral collection length and the radius of the implant extend beyond the pixel boundary, this analysis yields incorrect results. To mitigate these complications, the LWIR HgCdTe detector finite element model, which includes the wavelength and F/# number variables, is used to estimate the lateral collection length.

Detector responsivity, which is directly related to detector quantum efficiency, is measured for several detector implant diameters at each proton fluence. The corresponding lateral collection length is determined from the LWIR HgCdTe detector's finite element model. The relative responsivity versus lateral collection diode implant diameter is plotted for a number of different lateral collection lengths for a banded detector array with a pre-radiation lateral collection length of approximately 18 μm using both the finite element model output and measured data. The measured data is in close agreement with the model

prediction. The pre-radiation lateral collection length for these LWIR HgCdTe detectors is reported [17] to be in the range of 15 to 20 μm . Independent measurement of the lateral collection length validates this pre-radiation value [2]. As previously described, it is difficult to determine the absolute lateral collection length from the measured responsivity versus implant diameter data from the banded detector arrays because of: 1) the interaction between the micro-lens array and the lateral collection diodes, and 2) the limited extent of the pixels. It is important to note that this analysis will show the change of the lateral collection length as a function of proton fluence, but will not provide a high accuracy measure of its value.

1) *Damage Constants and Factors:* The change in LWIR HgCdTe detector performance in a proton environment is characterized by defining a damage constant or a damage factor. The damage constant describes the change in fundamental material parameters produced by a given fluence at a given energy. Damage factors are similar except they characterize the observed radiation degradation of a detector performance parameter such as responsivity or sensitivity. For this analysis, damage constants/factors for the lateral collection length and 14 μm implant detector responsivity are reported. It should be noted that the responsivity damage factors and the lateral collection length damage constant should have similar energy dependencies.

The lateral collection length damage factor can be computed from the measured lateral collection length as a function of proton fluence data. The lateral collection length is given by $L = \sqrt{D\tau}$, where D is the diffusion constant and τ is the minority carrier lifetime. The lateral collection length is related to the incident proton fluence by

$$\frac{1}{L^2} = \frac{1}{L_0^2} + K_L \Phi_P \quad (3)$$

where L_0 is the pre-radiation lateral collection length, K_L is the lateral collection length damage constant, and Φ_P is the proton fluence. The lateral collection length damage constant is determined from the slope of the line formed by plotting the inverse of the square of the measured lateral collection length versus proton fluence data. This procedure is repeated at each of the measured proton energies of 7, 12, and 63 MeV, and the resulting damage factors are compared with the NIEL energy dependence.

The responsivity damage factor, which is the change in responsivity per unit proton fluence, can be computed from the measured responsivity as a function of proton fluence. The change in responsivity is related to the incident proton fluence by

$$\Delta\text{Responsivity}(E) = K_R(E)\Phi_P(E) \quad (4)$$

where $K_R(E)$ is the responsivity damage factor and Φ_P is the proton fluence. Responsivity damage factors are computed for the 14 μm implant diameter detectors.

The responsivity damage factor is scaled to NIEL using a constant, R , which has units of responsivity change per unit of non-ionizing energy deposited as given by

$$K_R(E) = R \cdot \text{NIEL}(E). \quad (5)$$

2) *Performance Predictions Based on Measured Damage Factors*: The change in the on-orbit detector lateral collection length can be calculated by knowledge of the proton energy spectrum at the LWIR detector, which is typically found by transporting a proton spectrum at a given orbit through spacecraft shielding. The resultant proton spectrum at the detector is integrated with the energy dependence of the NIEL. The result of this calculation is then scaled to convert the NIEL energy dependence to the proper units of the damage constant. This process is given by

$$\begin{aligned} \Delta \left(\frac{1}{L_D^2} \right) &= \int_{E_1}^{E_2} K_L(E) \frac{d\Phi(E)}{dE} dE \\ &= L \int_{E_1}^{E_2} \text{NIEL}(E) \frac{d\Phi(E)}{dE} dE \end{aligned} \quad (6)$$

where $K_L(E)$ is the energy dependence of the lateral collection length damage function, $d\Phi(E)/dE$ is the differential proton spectrum, $\text{NIEL}(E)$ is the energy dependence of the NIEL in HgCdTe in units of $(\text{MeV} - \text{cm}^2)/g$, and L is the scaling factor between NIEL and the lateral collection length damage constant. This analysis assumes that displacement damage is linear with proton fluence, and that damage in the detectors has the same energy dependence as NIEL.

The change in the on-orbit detector responsivity can be calculated by integrating the product of proton energy spectrum at the detector and responsivity damage factor. The result of this calculation is then scaled to convert the NIEL energy dependence to the proper units of the responsivity damage factor. This process is described by

$$\begin{aligned} \Delta \text{Responsivity} &= \int_{E_1}^{E_2} K_R(E) \frac{d\Phi(E)}{dE} dE \\ &= R \int_{E_1}^{E_2} \text{NIEL}(E) \frac{d\Phi(E)}{dE} dE \end{aligned} \quad (7)$$

where $K_R(E)$ is the energy dependence of the responsivity damage factor and R is the scaling factor between NIEL and the responsivity damage factor.

IV. EXPERIMENT RESULTS AND ANALYSIS

A. Banded Detector Array Responsivity Characteristics Versus Implant Diameter

The measured detector responsivity as a function of implant diameter for the banded detector array is shown in Fig. 4. These data demonstrate that the measured responsivity (and therefore the detector current) increases as a function of the implant diameter as predicted by (3) and varies by 20% from the smallest to the largest implant diameter. Fig. 5 shows the detector array responsivity operability and the uncorrected responsivity nonuniformity (sigma/mean) as a function of implant diameter. The responsivity operability exhibits a general improvement with increasing implant diameter that corresponds to the improved uniformity with increasing implant diameter. The uniformity

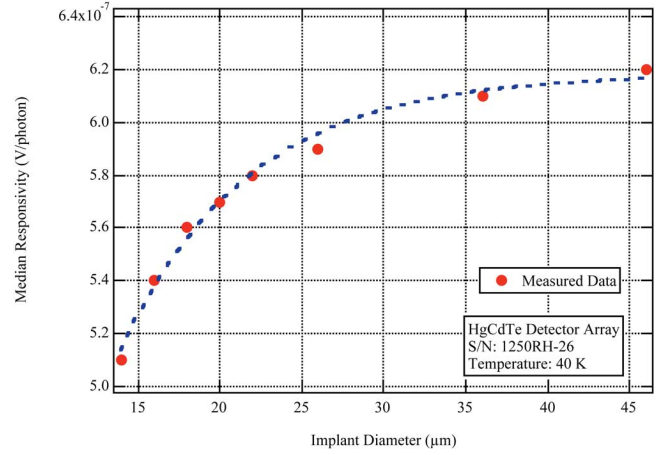


Fig. 4. LWIR HgCdTe detector array responsivity versus implant diameter.

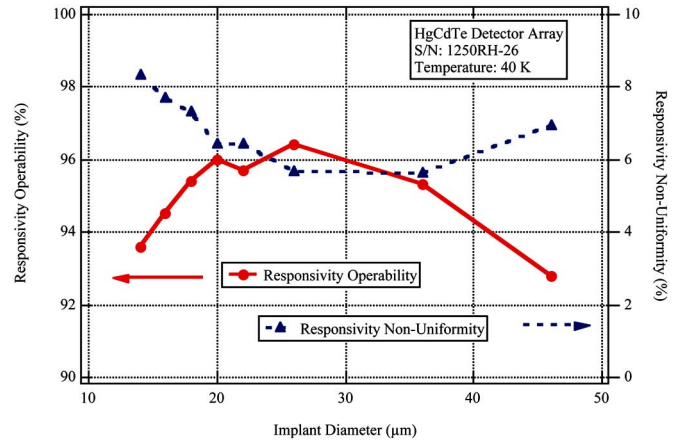


Fig. 5. LWIR HgCdTe detector array responsivity operability and nonuniformity versus implant diameter.

improves with increasing implant diameter because the pixel responsivity does not depend as strongly on lateral collection. This trend is valid for implant diameters smaller than $30 \mu\text{m}$; however, for implant diameters greater than $30 \mu\text{m}$ the responsivity operability decreases because the probability of the implant intersecting a defect (of the type known to be pervasive in the HgCdTe system, which results in inoperable pixels) increases with implant diameter. These responsivity operability data demonstrate that the optimal implant diameter for this pixel pitch is in the range of 20 to $30 \mu\text{m}$. These data further illustrate the tradeoff that occurs between performance and operability, and show that the detector design with larger diameter implants has higher overall responsivity; however, the detector design with the smaller implants, in general, has a higher number of operable detectors.

B. Detector Array Proton Radiation Characterization Data

1) Responsivity Characteristics at Proton Energy of 63 MeV:

Fig. 6 shows the median responsivity of the pixels with eight different implant diameters as a function of proton fluence. It is evident that all pixel designs exhibit a monotonic decrease in responsivity with increasing proton fluence and that the pixels with the smaller implant diameter exhibit the greatest

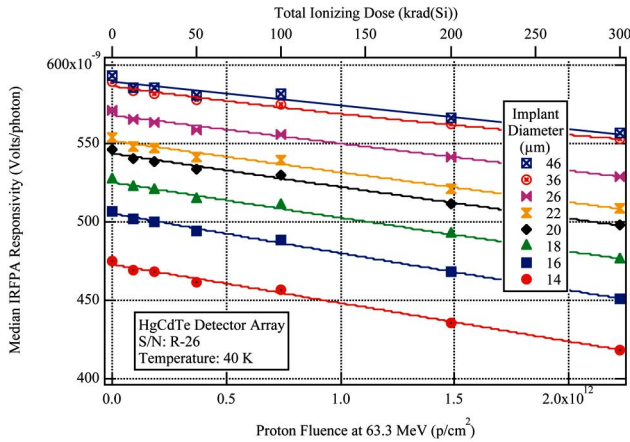


Fig. 6. Median responsivity versus proton fluence at 63 MeV.

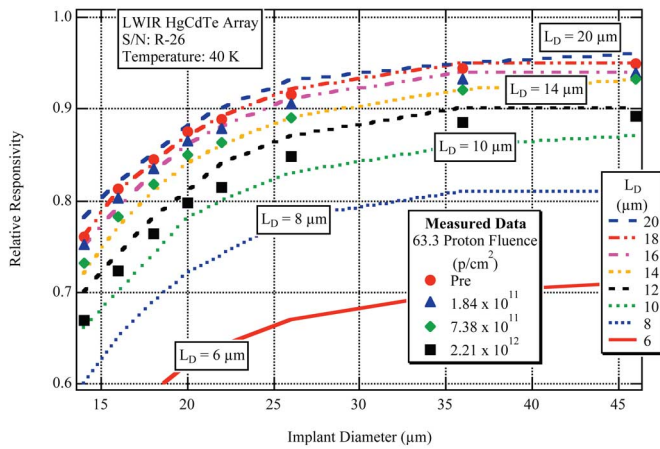


Fig. 7. Relative responsivity versus implant diameter at different 63 MeV proton fluences.

relative decrease in responsivity with proton fluence. The detector with the largest implant diameter (46 μm) exhibits a responsivity change of -6% at the highest proton fluence of $2.2 \times 10^{12} \text{ p/cm}^2$ at 63 MeV. In comparison, the detector with the smallest implant diameter (14 μm) exhibited a responsivity change of -14% at the same proton fluence, which corresponds to a responsivity damage factor of $2.4 \times 10^{-20} \text{ V/ph/p/cm}^2$.

As previously outlined, an estimate of the lateral collection length at each proton fluence can be made from these data by plotting the measured responsivity, normalized to the responsivity of the pixel with the largest implant diameter, versus the implant diameter. The responsivity of the pixel with the largest implant diameter is the least dependent on the lateral collection length. The lateral collection length can then be estimated by correlating these measured data with the detector finite element model that predicts the detector responsivity as a function of lateral collection length.

This process was followed, as shown in Fig. 7, and the lateral collection length was estimated at each proton fluence. Fig. 8 shows the lateral collection length versus proton fluence obtained from this process. These data show that the lateral collection length decreases by almost a factor of two at the highest proton fluence of $2.2 \times 10^{12} \text{ p/cm}^2$ at 63 MeV.

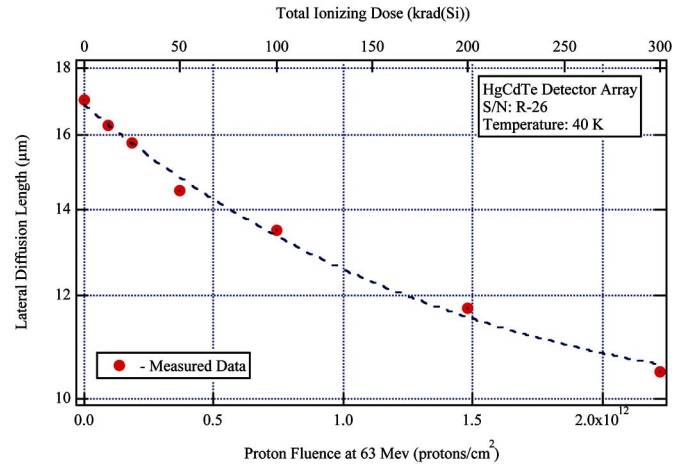


Fig. 8. Lateral collection length versus 63 MeV proton fluence.

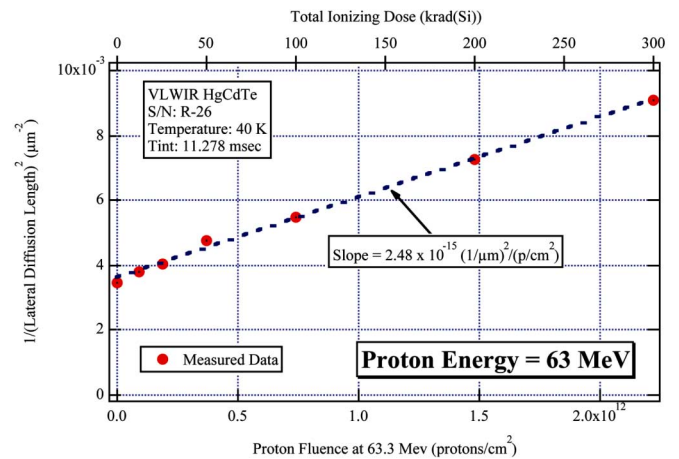


Fig. 9. Lateral diffusion length radiation damage factor analysis at 63 MeV.

Fig. 9 shows the inverse of the square of the estimated lateral collection length versus proton fluence. The slope of this line yields the lateral collection length damage factor, which is $2.5 \times 10^{-15} (1/\mu\text{m}^2)/(\text{p/cm}^2)$ at a proton energy of 63 MeV. Recall that this lateral collection length damage factor will be determined as a function of proton energy and will serve as the basis for developing an on-orbit performance model for estimating the change in responsivity of LWIR HgCdTe detector arrays as a function of on-orbit time.

2) *Responsivity Characteristics at Proton Energies of 12 and 7 MeV:* Responsivity measurements were also performed at proton energies of 12 and 7 MeV. These measurements are summarized in Table I, which also includes the measured results at proton energy of 63 MeV. Table I presents the proton measurement energy, the proton fluence at which the 14 μm implant diameter detector responsivity has decreased by 25%, the computed responsivity damage factor, and the lateral collection length damage factor. This table was generated by analyzing the measured data at each proton energy to determine the change in detector responsivity and the change in lateral collection length as a function of proton fluence.

The measured data at proton energies of 12 and 7 MeV exhibited similar characteristics to the measured data collected at

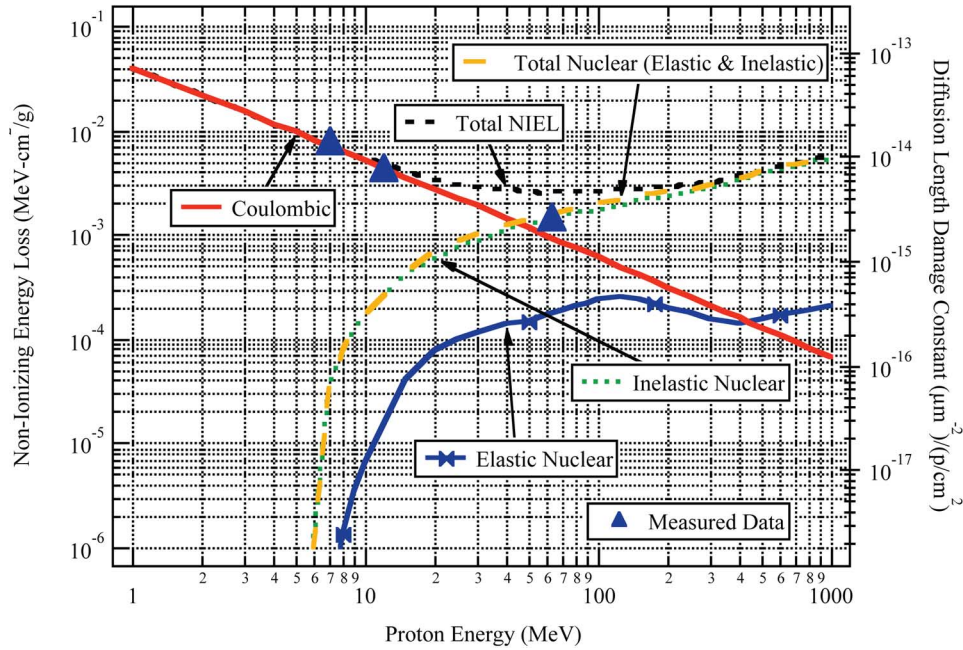


Fig.10. Energy dependence of measured lateral diffusion length damage constant compared to NIEL energy dependence.

 TABLE I
 SUMMARY OF MEASUREMENTS VERSUS PROTON FLUENCE

PROTON ENERGY (MeV)	PROTON FLUENCE WHERE CHANGE IN 14 μm IMPLANT DIAMETER DETECTOR RESPONSIVITY = -25 % (p/cm^2)	RESPONSIVITY DAMAGE FACTOR ($\text{V}/\text{ph}/\text{p}/\text{cm}^2$)	LATERAL COLLECTION LENGTH DAMAGE FACTOR ($(1/\mu\text{m}^2)/(\text{p}/\text{cm}^2)$)
7	9.9×10^{11}	1.2×10^{-19}	1.3×10^{-14}
12	1.4×10^{12}	8.6×10^{-20}	7.0×10^{-15}
63	5.0×10^{12}	2.4×10^{-20}	2.5×10^{-15}

a proton energy of 63 MeV. The measured data at proton energies of 12 and 7 MeV demonstrated that each pixel design exhibited a monotonic decrease in responsivity with increasing proton fluence, and that the pixels with the smaller implant diameter exhibit the greatest relative decrease in responsivity with increasing proton fluence.

Measured data collected at a proton energy of 12 MeV from the detector with the smallest implant diameter (14 μm) demonstrate a change in detector responsivity of -13% at a proton fluence of 6.2×10^{11} p/cm^2 , which corresponds to a responsivity damage factor of 8.6×10^{-20} $\text{V}/\text{ph}/\text{p}/\text{cm}^2$. These 12 MeV proton data were further analyzed to determine the lateral collection length as a function of proton fluence. This analysis yields a lateral collection length damage factor of 7.0×10^{-15} $(1/\mu\text{m}^2)/(\text{p}/\text{cm}^2)$.

At 7 MeV, the detector with the 14 μm implant diameter exhibits a change in responsivity of -12% at a proton fluence of 4.2×10^{11} p/cm^2 , which corresponds to a responsivity damage factor of 1.2×10^{-19} $\text{V}/\text{ph}/\text{p}/\text{cm}^2$. Subsequent analysis of these data determined the lateral collection length damage factor to be 1.3×10^{-14} $(1/\mu\text{m}^2)/(\text{p}/\text{cm}^2)$.

V. DISCUSSION

This section presents the measured lateral collection length damage constant and responsivity damage factors correlated to

the calculated proton NIEL in HgCdTe. The energy dependence of the NIEL provides a framework for estimating the on-orbit performance of these parameters.

This correlation methodology made two assumptions that required validation to provide confidence in this analysis. The first assumption was that change in detector performance was due to displacement damage and that this change was linear with proton fluence. This first assumption has been validated with the measurement results as summarized in Table I. The second assumption was that the lateral collection length and responsivity changes in the detectors have the same energy dependence as NIEL. The second assumption is tested by comparing the energy dependence of the lateral collection length damage factors to the NIEL energy dependence as shown in Fig. 10 and Fig. 11. These measured data show a monotonic decrease in both the lateral collection length damage constant and the responsivity damage factor with energy at the lower proton energies of 7 and 12 MeV. At 63 MeV, the lateral collection length damage factor continues to decrease, but not at the rate predicted by the Coulombic contribution to the NIEL. This is likely due to the increase in the inelastic damage contribution to the total NIEL above proton energies of 30 to 50 MeV. The measured data at 63 MeV does not exactly correspond to the calculated NIEL; if the NIEL curve were used to predict the on-orbit change in detector responsivity, it would provide a conservative estimate of the performance change.

It is interesting to note in this interpretation that an apparent weighting factor less than unity seems to apply to the damage resulting from nuclear collisions for the purpose of minority carrier diffusion, and we note that deviations from linearity with total damage may be expected, or at least explained in some circumstances. In this case, our first-order picture of the mechanism responsible for photo-generated charge being collected at the pixel's depletion region relies substantially on diffusion plus

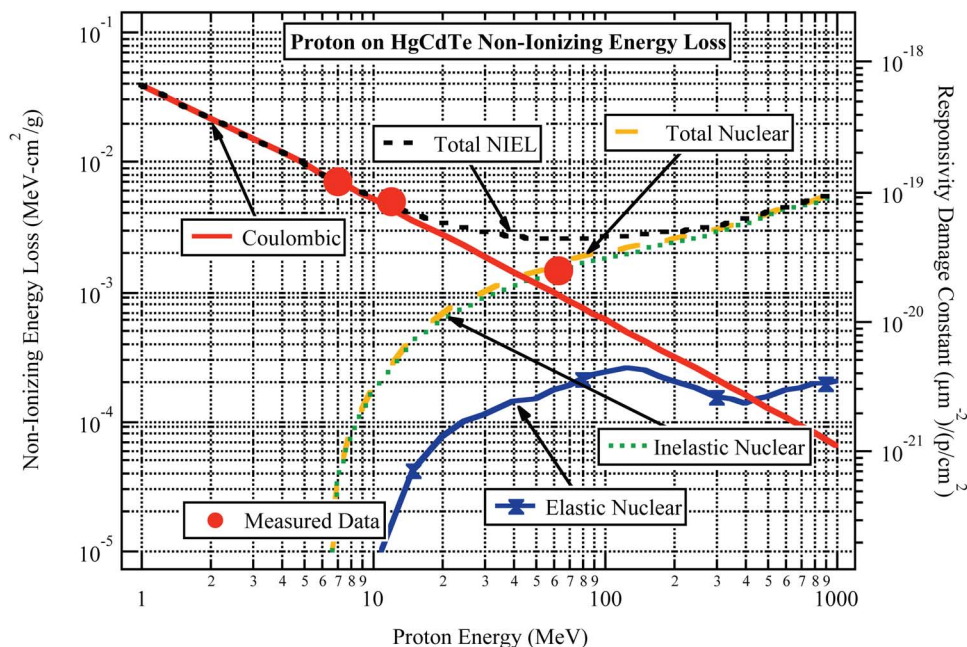


Fig. 11. Energy dependence of responsivity damage factor compared to NIEL energy dependence.

drift-assisted diffusion where fields are present. Charge generation occurs uniformly across the area of the pixel, and only those carriers that diffuse to the central junction are collected. With this in mind, we note that proton damage from Coulombic scattering is uniformly and homogeneously distributed as point defects throughout the pixel volume. We suggest that when nuclear collisions are responsible for damage, which is present as highly localized subcluster regions, there may be self screening of recombination centers in highly disordered regions. This nonlinearity with damage morphology may lead to the observed deviation of the damage factor with NIEL at the higher energy where nuclear reactions impart the majority of total damage, but only in high energy collisions where subclusters are expected. Further work in modeling, as well as experimental results at higher energies, will be required to fully understand this relationship, and we suggest that the use of the NIEL energy dependence to describe the minority carrier damage factor may be appropriate as a conservative upper bound if measurements are made at low energies where Coulomb mechanisms dominate. Caution is advised if only high energy data are available, as underestimation of the total damage from a shielded spectrum may be possible.

VI. SUMMARY

This study investigated the change in performance of LWIR HgCdTe detector arrays in a proton environment. Data have been presented that describe the responsivity characteristics of LWIR HgCdTe detector arrays as functions of proton fluence at proton energies of 7, 12, and 63 MeV. Measured data show that the LWIR HgCdTe detectors exhibit a monotonic decrease in responsivity with increasing proton fluence. At each proton fluence, the lateral collection length was estimated by correlating measured data with a detector finite element model that predicts the detector responsivity as a function of lateral collection

length. The plot of the inverse of the square of the lateral collection length versus proton fluence was used to determine the lateral collection length damage factor at proton energies of 7, 12, and 63 MeV. The energy dependence of the lateral collection length damage factors shows a monotonic decrease with energy at the lower proton energies of 7 and 12 MeV. At 63 MeV, the lateral collection length damage factor continues to decrease at a rate less than that predicted by the Coulombic contribution to the NIEL. This difference from the prediction is likely due to the increase in the inelastic damage contribution to the total NIEL above proton energies of 30 to 50 MeV. These measured data support the assumptions that that displacement damage is linear with proton fluence and that the lateral collection length damage factor in LWIR HgCdTe detectors can be approximated by the energy dependence of NIEL. To further validate this approach, measured data at proton energies between 12 and 63 MeV, and also at proton energies greater than 100 MeV, is highly desirable. These results provide the basis for the development of an on-orbit performance model.

This study represents findings of the first experimental investigation to assess the proton energy dependence of LWIR HgCdTe minority carrier diffusion length degradation resulting from proton damage. The energy dependence of measured damage factors is compared with calculations of the NIEL in LWIR HgCdTe, and our results indicate both that proton-induced displacement damage may seriously degrade detector performance, and that NIEL energy dependence can be used with care for hardness assurance assessment of performance in an orbital proton environment.

REFERENCES

- [1] P. W. Marshall, J. E. Hubbs, D. C. Arrington, C. J. Marshall, R. A. Reed, G. Gee, J. C. Pickel, and R. A. Ramos, "Proton-induced transients and charge collection measurements in a LWIR HgCdTe focal plane array," *IEEE Trans. Nucl. Sci.*, vol. 50, no. 6, pp. 1968–1973, Dec. 2003.

- [2] J. Hubbs, D. Arrington, M. Gramer, G. Dole, and R. Ramos, "Proton and total dose characterization of LWIR focal plane arrays that utilize micro-lens detectors," presented at the 2003 Military Sensing Symposium Specialty Group on Infrared Material and Detectors, Tucson, AZ.
- [3] B. C. Fodness, P. W. Marshall, R. A. Reed, T. M. Jordan, J. C. Pickel, I. Jun, M. A. Xapsos, E. A. Burke, and R. Ladbury, "Monte Carlo treatment of displacement damage in bandgap engineered HgCdTe detectors," in *Proc. 7th Eur. Conf. Radiation and its Effects on Components and Systems*, 2003, pp. 479–485.
- [4] J. F. Ziegler, J. P. Biersack, and U. Littmark, *The Stopping and Range of Ions in Solids*, J. F. Ziegler, Ed. New York: Pergamon Press, 1985, vol. 1, Stopping and Ranges of Ions in Matter.
- [5] S. R. Messenger, E. A. Burke, M. A. Xapsos, G. P. Summers, R. J. Walters, I. Jun, and T. M. Jordan, "NIEL for heavy ions: An analytical approach," *IEEE Trans. Nucl. Sci.*, vol. 50, no. 6, pp. 1919–1923, Dec. 2003.
- [6] I. Jun, "Effects of secondary particles on the total dose and the displacement damage in space proton environment," *IEEE Trans. Nucl. Sci.*, vol. 48, no. 1, pp. 162–175, Feb. 2001.
- [7] "MCNPX User's Manual: Version 2.4.0," Los Alamos National Lab., Sep. 2002, LA-CP-02-408.
- [8] I. Jun, M. A. Xapsos, S. R. Messenger, E. A. Burke, R. J. Walters, G. P. Summers, and T. M. Jordan, "Proton NonIonizing Energy Loss (NIEL) for device applications," *IEEE Trans. Nucl. Sci.*, vol. 50, no. 6, pp. 1924–1928, Dec. 2003.
- [9] P. W. Marshall and C. J. Marshall, "Proton effects and test issues for satellite designers," in *IEEE NSREC Short Course*, Norfolk, VA, 1999.
- [10] P. W. Marshall, C. J. Dale, and E. A. Burke, "Proton-induced displacement damage distributions and extremes in silicon microvolumes," *IEEE Trans. Nucl. Sci.*, vol. 37, no. 6, pp. 1776–1783, Dec. 1999.
- [11] W. McLevige, "HgCdTe double layer planar heterostructure detectors for tactical and strategic applications," presented at the 1995 Military Sensing Symp. Specialty Group on Infrared Material and Detectors, Gaithersburg, MD, 1995.
- [12] W. McLevige, "Application of lateral collection concepts in LWIR HgCdTe double planar heterostructure detectors," presented at the 1996 Infrared Information Society Specialty Group on Infrared Material and Detectors, Boulder, CO, 1996.
- [13] W. McLevige, "Performance of LWIR HgCdTe focal plane arrays for low background 40 K strategic applications," presented at the 1997 Infrared Information Society Specialty Group on Infrared Material and Detectors, Monterey, CA, 1997.
- [14] W. McLevige, "Improved uniformity of small area LWIR HgCdTe diodes for 40 K strategic focal plane arrays," presented at the 1999 Infrared Information Society Specialty Group on Infrared Material and Detectors, Lexington, MA, 1999.
- [15] D. Lee, "Modeling of optical response in graded absorber layer detectors," presented at the 2006 Military Sensing Symposium Specialty Group on Infrared Material and Detectors, Orlando, FL, 2006.
- [16] C. M. Castaneda, "Crocker Nuclear Laboratory (CNL) radiation effects measurement and test facility," in *Proc. 2001 IEEE Radiations Effects Data Workshop*, 2001, pp. 77–81.
- [17] D. Lee, private communication Teledyne Imaging Systems, Camarillo, CA, May 2006.